Detecting persistent regimes in the North Atlantic Oscillation time series

Vidunas, Raimundas
Mathematics Department, Kyushu University

出版情報：MHF Preprint Series. 2006-12, 2006-03-16. 九州大学大学院数理学研究院
バージョン：
権利関係：

MHF Preprint Series

Kyushu University
21st Century COE Program
Development of Dynamic Mathematics with High Functionality

Detecting persistent regimes in the North Atlantic Oscillation time series

R. Vidūnas

MHF 2006-12

(Received March 16, 2006)

Faculty of Mathematics
Kyushu University
Fukuoka, JAPAN

Detecting persistent regimes in the North Atlantic Oscillation time series

Raimundas Vidunas
Kyushu University,
Mathematics Department

March 15, 2006

1 Introduction

The North Atlantic Oscillation (NAO) is a dominant factor of atmospheric variability in the Northern hemisphere, characterized by the (anti)correlation of weather patterns between the Arctic and the subtropical Atlantic, primarily in the winter season. It is determined by swings in the atmospheric sea level pressure difference between the Arctic and the subtropical Atlantic. If the subtropical high pressure (say, in Azores) and Arctic low pressure (in Iceland) are enhanced, westerly cyclone paths are dominant, resulting in warm wet winters in Europe and the Eastern US, but cold and dry winters in Greenland and Northern Canada. With the opposite pressure difference, westerly winter storms are rare, with the effect of cold winter in Europe and the Eastern US, but mild winters in Greenland. This weather pattern was noticed already by seafaring Scandinavians centuries ago.

The phase of the North Atlantic Oscillation affects intensity and number of Atlantic storms, their paths, ocean currents, heat content and ice cover, agricultural harvests, fishery yields. There is a big research interest in understanding the North Atlantic Oscillation, its history and predictability, its role in a global climate change, its interaction with the ocean and other climate agents.

The time series of the NAO indices are usually analyzed by spectral or wavelet methods [6]. A less conventional working hypothesis is that the NAO alternates between several stable *regimes* or *climate types or modes*. A related hypothesis is that *regime shifts* occur that separate periods of different character.

In this paper we apply straightforward statistical methods to determine possible stable regimes of the North Atlantic Oscillation. We use the Winter (December

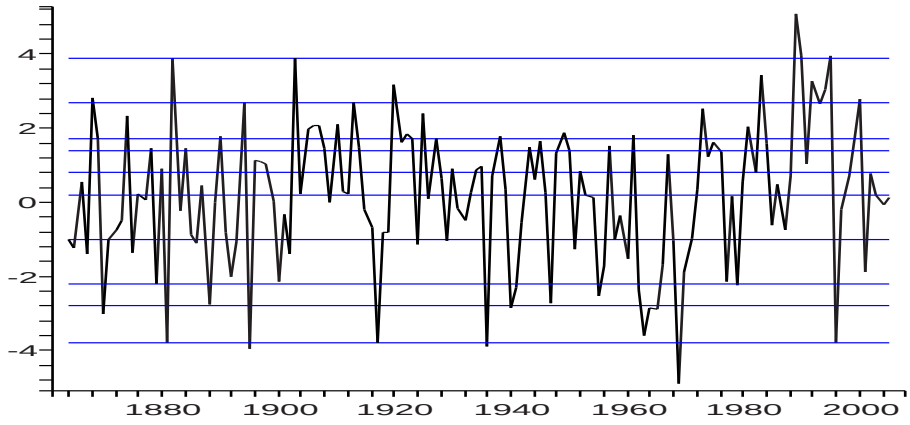

Figure 1: Hurrell's NAO time series.

through March) Station Based NAO Index time series of Hurrell [3], which the data available from the winter of 1863–1864. The values are differences between normalized seasonal mean Sea Level Pressures between Lisbon (Portugal) and Stykkisholmur/Reykjavik (Iceland). The seasonal mean pressures are normalized by dividing them by the long-term mean (1864-1983) standard deviation; this is done to avoid the series being dominated by the greater variability of the northern station.

It this paper, we primarily investigate the distribution of the NAO index values throughout the period 1864–2005. The distribution appears to be distinctly unlike the Gaussian normal distribution, with several steep peaks. The peaks suggest persistent regimes (climate types) that correspond to the preferred oscillating values of the NAO time series. Presumably, these values represent attractors or Lagrangian points of the underlying dynamical system.

Since there is no canonical way to represent distribution of a finite set of empirical data values, it is difficult to present one convincing graph of the distribution, or determine the persistent values with high precision. We will present distribution graphs in Section 2. Here we present the set of the persistent NAO values that we distinguish, determined up to one digit after the decimal point:

$$\Sigma = \{-3.8,\ -2.8,\ -2.2,\ -1.0,\ 0.2,\ 0.8,\ 1.4,\ 1.7,\ 2.7,\ 3.9\}. \tag{1}$$

In Figure 1, we present Hurrell's NAO time series by the bold curve, and these 10 values by horizontal blue lines. To appreciate persistence of these values, note that the bottom line is hit by 5 spikes from above, and nearly hit one more time in 1963,

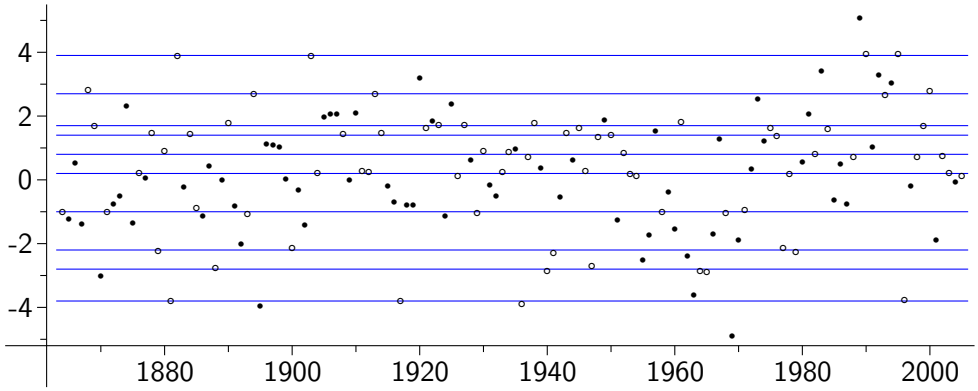

Figure 2: The North Atlantic Oscillation

while other closest values are in the vicinity of the second lowest line, or the lonely point way below. Similarly, the uppermost line is hit 4 times (in 1990 as well), while there is only one value clearly higher. We can check this observation by inspecting the monotonically ordered sequence of all NAO values:

$$-4.89, -3.97, -3.89, -3.80, -3.80, -3.78, -3.60, -3.01, -2.88, \ldots$$
$$\ldots, 3.03,\ 3.18,\ 3.28,\ 3.42,\ 3.87,\ 3.89,\ 3.96,\ 3.96,\ 5.08.$$

There is clearly concentration of NAO values around -3.8 and 3.9, with large gaps immediately before and after these marks.

Figure 2 is an alternative presentation of the NAO time series, together with the blue horizontal lines of the persistent values. The NRO value of each year is represented by a circle or a disc of radius 0.10 (in the vertical scale). The values which are within 0.11 of any value in the set Σ are represented by circles, the other values — by filled discs. The number of values of both kinds is the same: half of the values are represented by circles, and half — by filled discs.

If we count the NAO values which lie within 0.10 of any value in the set Σ, there are 67 (out of 142) such values. This is 47% of all values, while the neighborhoods with the radius 0.10 cover about 20% of the variation interval. If we adjust the persistent values in Σ up to two digits after the decimal point, we can have more than half of all values within 0.10.

This analysis works only with the set of NAO values, and disregards their temporal order. In Section 3 we investigate the degree of dependance of consecutive NAO

values, primarily by considering the distribution of pairs of NAO values of consecutive years. When the pairs of consecutive NAO values are plotted as points in the Cartesian plane, we can distinguish many lines which go nearby remarkably many (or remarkably few) plotted points. This observation suggests not only "attractor" regimes, but also dominant linear regressions (of first order) for climate transitions from year to year. Apparently, different dynamical mechanisms dominate transitions between different years, but there might be a few most frequently occurring transitional modes. We list the most probable linear regressions. Further analysis may show which linear regressions are more likely to be substantial, or how they change throughout decades.

2 The NAO value distribution

A simple way to represent the distribution of a finite set of real values by a continuous function is to model the contribution of a single value by the Gaussian normal distribution with a small standard deviation, centered at that value. All contributions have to summed up and divided by the number of values — this is a case of *Parzen density estimation with a Gaussian kernel*, which a form of *radial basis expansion* and a *mixture model for density estimation* [1, Sections 6.6–6.8]. More specifically, let $\mathcal{S}$ denote a sequence $(z_1, z_2, \ldots, z_N)$ of real numbers, and let σ_0 denote a real number. We introduce the function

$$F(\mathcal{S}, \sigma_0; x) = \frac{1}{\sqrt{2\pi}\,\sigma_0 N} \sum_{j=1}^{N} \exp\left(-\frac{(x - z_j)^2}{2\,\sigma_0^2}\right). \tag{2}$$

We consider this function as a continuous approximant for the distribution function for the discrete set $\mathcal{S}$. The contribution of each member of $\mathcal{S}$ is modelled by the Gaussian distribution with the standard deviation σ_0, and the cumulative distribution functions is the sum of contributions divided by N. Clearly, the integral of $F(\mathcal{S}, \sigma_0; x)$ over the real line is equal to 1.

Let $\mathcal{H}$ denote the sequence of Hurrel's NAO values. The left-hand side of Figure 3 depicts $F(\mathcal{H}, 0.10; x)$, by the bold black graph. The red graph depicts the approximating Gauss normal distribution of $\mathcal{H}$; the mean and standard deviation of the Gaussian graph are respectively equal to the mean and standard deviation of all values of $\mathcal{H}$. The vertical lines represent the 10 persistent values presented in (1).

As we see, the modelled distribution differs significantly from the approximating Gauss normal distribution. There are many significant peeks and dips, the black curve oscillates around the red one wildly. The stark deviation from the Gauss normal distribution must have underlying reasons.

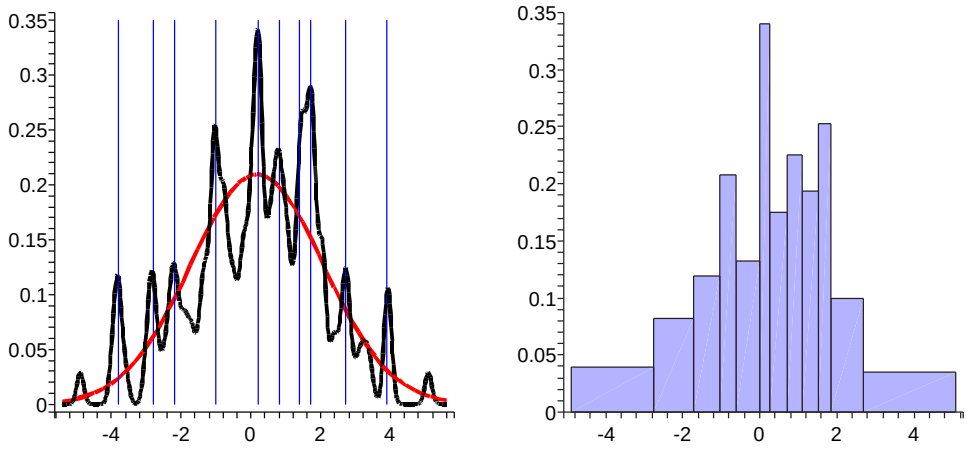

Figure 3: Distribution of the NAO index values

The high peaks of $F(\mathcal{S}, \sigma_0; x)$ can be clearly distinguished. Location of those peaks suggests clear candidates for a conjectural set of persistent NAO values. The distinguishable values are those presented in (1). Only the maximum at 1.4 is not clearly distinguishable from the nearby peak at 1.7, but investigation by other means (say, the same kind of graph with $\sigma_0 < 0.10$) confirms significance of the value 1.4.

Alternatively, one may model a distribution for a finite set of data values by drawing histograms. But histograms are notoriously unstable with respect to the choice of boundaries of tallied classes. Fixed width histograms may depend drastically on the choice of the variation interval and the number of bars.

We prefer to consider histograms where tallied classes are subdivided by equally spaced quantiles. When the bars are drawn of equal area, their height models the distribution well. Such histograms can be routinely drawn with Maple's command statplots[histogram]. For a value set $\mathcal{S}$ and a positive integer m, let $G(\mathcal{S}, m; x)$ denote the histogram function with the tallied classes subdivided by the p-quantiles, where $p = j/m$ with $j = 0, 1, 2, \ldots, m$.

The right hand side of Figure 3 depicts $G(\mathcal{H}, 12; x)$. The histogram does not look like a Gauss normal distribution at all. Surely, quantile histograms depend drastically on the chosen number of intervals; they are also very unstable when new data is added. But we can consider an assortment of many histograms $G(\mathcal{H}, m; x)$, with various m. We are particularly interested in local maxima of these histograms. The maxima are expected to cover actual persistent values consistently. Figure 4

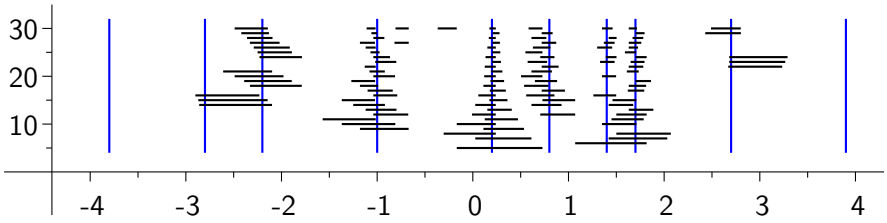

Figure 4: Local maxima of quantile histograms

depicts the local maxima of these histograms, with m varying from 5 to 30 (the vertical axis). We see that most of the chosen values in (1) indeed fall on the local maxima. In particular, we can observe the splitting of close persistent values 1.4 and 1.7. Longer intervals are actually less significant relatively, since (for fixed m) sharper maximums correspond to shorter intervals. The staircase or tree-like patterns around the Σ-values $-2.2, -1.0, 0.2$ have arithmetic origin. For instance, the Σ-value 0.2 is very close to the median value 0.24, so the local maximum for even n consistently ends at 0.24, while for odd n the median value is inside the interval of the extremum. The Σ-value -1.0 is very close to the first quartile.

Yet another alternative for delimiting persistent values is to consider shortest intervals containing a certain number n of observed values. Persistent values are expected to be covered by the short intervals for various n. Shortest intervals are more intrinsically defined than maxima locus of histograms. They are more stable when new data is added, and do not depend on quantile arithmetic. On the other hand, "locally" minimal intervals can intersect each other, so it is tricky to depict them. Instead of defining strictly which intervals are remarkably short, we tried a few reasonable algorithms to pick up and depict short intervals.

Figure 5 depicts short intervals with n values, with n varying from 4 to 40. The intervals were picked up and depicted following this algorithm:

1. Fix n, and start with an empty set Z of "picked up" intervals. Order the sequence of NAO values in the monotonic non-decreasing order. By an interval containing n values we mean an interval which starts at the j-th smallest NAO value, and ends at the $(j+n-1)$-th smallest value.

2. Consider the set X of all intervals containing n values which do not intersect intervals in Z, and do not contain the extremal values $5.08, -4.89$. But we allow the intervals in X to have common end-points with intervals from Z.

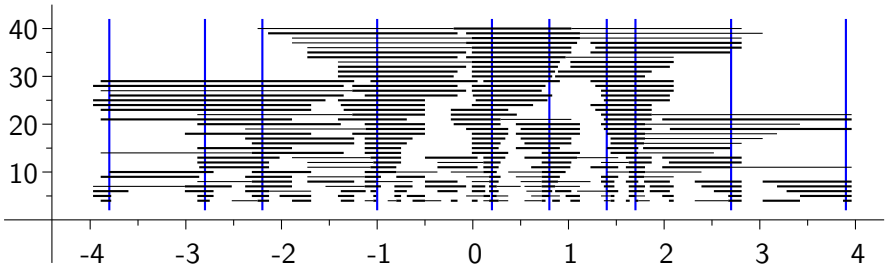

Figure 5: Shortest intervals with $n = 4, 5, \ldots, 40$ values

3. If X is empty, stop the algorithm. Otherwise choose an interval J from X of minimal length. If there are other intervals of the same length intersecting J, enlarge J to the union of these intervals.

4. If J does not have common end-points with intervals from Z, depict it by a bold line. If J has exactly one common point with some interval J' from Z, and J' was depicted by a bold line, depict J by a thin line. Otherwise do not depict J by any line.

5. Append J to Z, and go to step **2.**

There is indeterminacy in step **3.**, when there are several non-intersecting intervals of the same length, but it was not influential for the picture. This algorithm produces quite an ordered picture. Like in Figure 4, longer depicted intervals are usually less significant, but they may also represent union of equally short intervals (see Step **3.**) As we see, the picked up values are indeed consistently covered by the depicted intervals, at least for small enough n. Unsurprisingly, the short intervals for larger n frequently span the persistent values. The short intervals also have favored end-points, from where the NAO values start to concentrate to the left or to the right.

In conclusion, we tried to define or delimit the persistent NAO values by several methods: continuous distribution approximation, histograms, shortest intervals with many values. By each method, we can consistently and distinctly distinguish the same set (1) of persistent NAO values, except that the extremal persistent values $3.9, -3.8$ are not visible from the histograms; but these two values are clearly visible by the other 2 methods.

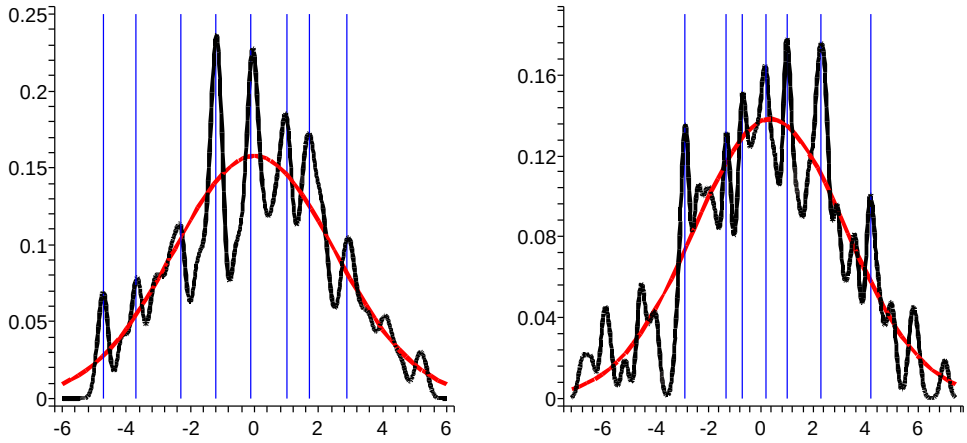

Figure 6: Distribution of differences and sums of consecutive NAO values

3 Distribution of consecutive values

In the previous Section, the temporal order of NAO values was disregarded. Here we consider the distribution of pairs of NAO values of consecutive years. We will notice indications that there exist persistent transitional modes between consecutive years, along with persistent constant regimes (1) considered in Section 2. In particular, we determine a bunch of most probable persistent first order linear regressions between consecutive NAO values.

First we take a look at distribution of differences and sums of consecutive NAO values. In other terms, we look how the jumps and two-year averages of NAO values are distributed. Recall that by $\mathcal{H}$ we denote the sequence of Hurrell's NAO values. For $k = 1864, 1865, \ldots, 2005$, let us denote the NAO value for the year k by a_k. Let $\mathcal{H}_2^-$ denote the sequence of differences $a_k - a_{k-1}$ of consecutive NAO values, and let $\mathcal{H}_2^+$ denote the sequence of sums $a_k + a_{k-1}$ of consecutive NAO values (with k varying from 1865 to 2005). Figure 6 depicts the graphs $F(\mathcal{H}_2^-, 0.15, x)$ and $F(\mathcal{H}_2^+, 0.15, x)$ for the distributions of consecutive differences and sums, together with the best approximating Gaussian distributions. There are actually a few outliers outside the plotted range: the difference values $7.67, -6.65, -7.74$, and the sum value 9.04. As we see, the distribution graphs deviate markedly from the respective Gaussian normal distributions. Just as in Figure 3, there are several distinguishable peaks and valleys.

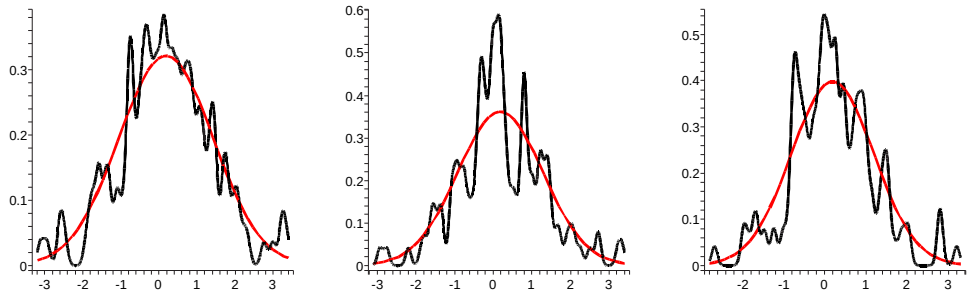

Figure 7: Distributions of 3-4-or-5 year averages of NAO values

The markedly persistent difference values are

$$\Sigma^- = (-4.7, -3.7, -2.3, -1.2, -0.1,\ 1.0,\ 1.7,\ 2.9). \tag{3}$$

The markedly persistent sum values are

$$\Sigma^+ = (-2.9, -1.3, -0.7,\ 0.2,\ 1.0,\ 2.3,\ 4.2). \tag{4}$$

Similarly, Figure 7 depicts the distribution graphs for 3-4-or-5 year averages of NAO values. More specifically, for a positive integer n let $\mathcal{H}_n$ denote the sequence of n-year averages of available NAO values. Figure 7 depicts the graphs $F(\mathcal{H}_3, 0.08, x)$, $F(\mathcal{H}_4, 0.07, x)$ and $F(\mathcal{H}_5, 0.07, x)$, together with the best approximating Gaussian distributions. We still observe stark deviations from the Gaussian distributions, and there is no sign of averaging the deviations out. This suggests that not only NAO values tend to concentrate around the marks in (1), but they are to some degree dependent. The values must be related, either by constant or usually present relations, or perhaps by an alternating set of persistent relations.

Let us look for first order linear regressions that possibly would relate consecutive NAO values often. The persistent jumps of NAO values in (3), or persistent two-year-sums in (4) offer a special kind of first order linear regressions. Let $\mathcal{P}$ denote the set of points (a_{k-1}, a_k) in the Cartesian plane; the points represent pairs of consecutive NAO values. The left-hand side of Figure 8 depicts the points of $\mathcal{P}$ by small circles, together with the horizontal or vertical blue lines showing the persistent NAO values (1), and the light blue lines showing the persistent differences (3) and sums (4) of consecutive NAO values. These lines are supposed to pass very close to remarkably many points of $\mathcal{P}$, most these points within the class of lines with the vertical, horizontal or $\pm 45^0$ slope. For comparison, on the right-hand side we

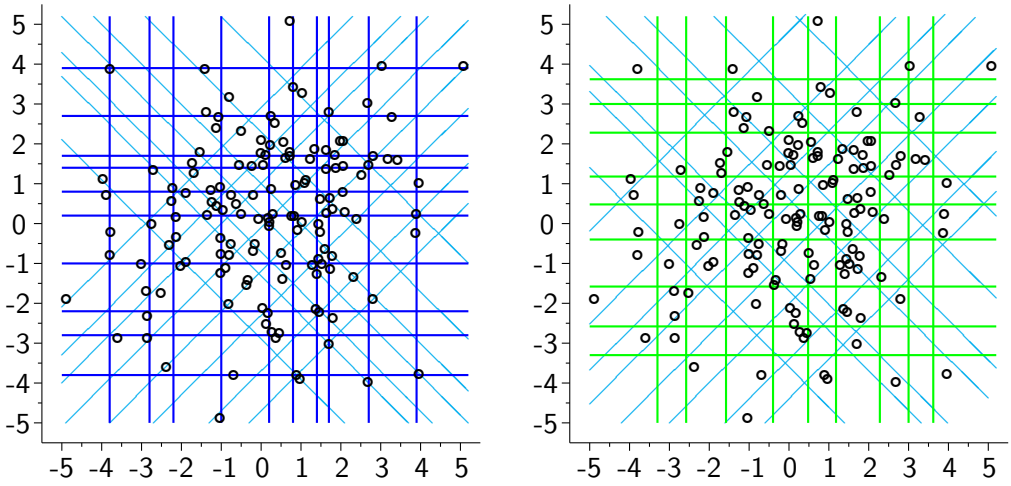

Figure 8: Pairs of consecutive NAO values

plot similar lines corresponding to the striking minima of the distribution graphs in Figures 3 (in green) and 6 (in light blue, again). Only a few points of $\mathcal{P}$ are close to these lines. There is a remarkable contrast between the two pictures in Figure 8.

One may notice in Figure 7 several instances of notable many points lying "more or less" on the same line of other slope than horizontal/vertical or $\pm 45^0$. To investigate more general first order linear regressions, we considered the sequences

$$\mathcal{H}^*_\alpha = \{(a_{k-1} - \widetilde{a}) \sin\alpha + (a_k - \widetilde{a}) \cos\alpha \ : \ k = 1865, 1866, \ldots, 2005\}\,, \qquad (5)$$

where $\widetilde{a} = 0.18$ is close to the average of all a_k's, and α varies through the discrete set $\{\pi j/120 \ : \ j = 0, 1, 2, \ldots, 119\}$. For each such α, we computed the values of $\mathcal{F}(\mathcal{H}^*_\alpha, 0.10, x)$, with the values of x spaced by 0.02. We found the local maxima of the $\mathcal{F}$-distributions, and then we considered only those maxima which are also local maxima with respect to α. With our algorithm, we got about 230 local maxima (after throwing out many maximal values less that 0.075, typically representing just one or two $\mathcal{H}^*_\alpha$-values most far away from $\widetilde{a}$). The regression lines defined by these local maxima should pass very close to more $\mathcal{P}$-points than "normally" expectable. To find most remarkable regression lines, we ordered the found maxima in two ways: by the extremal value itself, and by the the ratio of the extremal value to the distribution value expected from the respective approximating Gaussian normal distribution.

Then we tried to plot subsequently the regression lines against the points of $\mathcal{P}$.

The first 4 pictures in Figure 9 depict total 96 best looking regression lines plotted against the set $\mathcal{P}$. The lines were consequently picked up from the two ordered lists of local maxima in an alternating manner. Each new line was first plotted alone and in each of the 4 pictures under continuous build up, and if the line looked remarkable enough and aesthetically fitting in one of the 4 pictures, it was added to that picture. The most remarkable lines were preferably plotted in the top left picture, then top right picture, and so on. Here are the parameters (j, b) which define the plotted lines

$$(x - \widetilde{a}) \sin \frac{\pi j}{120} + (y - \widetilde{a}) \cos \frac{\pi j}{120} = b : \tag{6}$$

I : $(3, -3.96), (5, -2.28), (5, 0.04), (6, -1.06), (17, 1.68), (25, 2.98), (37, 0.86), (41, -0.08),$
$(43, -1.12), (57, -4.02), (60, 3.74), (-58, 2.92), (-58, 2.40), (-54, 0.28), (-53, -1.46),$
$(-41, -1.60), (-31, 0.66), (-12, -0.44), (-10, 0.62), (-8, 1.40), (0, 3.74);$

II : $(6, -2.88), (6, 1.88), (9, -0.88), (9, -0.04), (9, 3.24), (25, -4.72), (35, -0.44), (39, -1.40),$
$(45, 1.98), (52, 3.54), (54, -3.36), (54, 0.10), (56, -1.24), (-58, -1.36), (-51, -0.04),$
$(-50, 2.16), (-49, -3.60), (-38, 2.32), (-37, -1.84), (-36, -0.12), (-25, -2.56),$
$(-22, -0.44), (-20, 0.70), (-18, 1.46), (-9, -4.66), (-6, 0.26), (-2, 1.30);$

III : $(11, -2.68), (12, -0.78), (14, -1.76), (22, 2.10), (24, -0.14), (24, 1.22), (30, -2.28), (34, -0.74),$
$(40, 1.26), (43, 0.50), (47, -3.66), (55, 1.22), (56, 3.32), (57, -3.24), (60, 0.02), (-46, 0.62),$
$(-44, 2.14), (-44, 1.48), (-44, -0.92), (-34, -3.14), (-26, 0), (-24, 1.34), (-5, 1.48), (-1, 0);$

IV : $(1, -1.22), (12, 2.32), (18, -2.52), (19, -0.38), (27, -0.96), (32, 0.52), (42, -4.00), (42, -3.36),$
$(45, 1.06), (46, 3.36), (50, -0.64), (55, 1.92), (59, 0.64), (-57, 0.86), (-55, 2.02), (-47, -0.56),$
$(-41, 2.28), (-37, 1.08), (-31, -3.32), (-30, -0.84), (-18, -0.20), (-14, 1.18), (-12, -2.82),$
$(-2, 0.74).$

The plotted lines indeed appear to pass very close to notably many points. Remarkable instances of quite many points lying "more or less" on the same line are noticeable even if the line is not plotted.

For comparison, we considered the lowest local minima (both in x and α) of distribution functions $\mathcal{F}(\mathcal{H}^*_\alpha, 0.10, x)$ as well. These minima give lines which lie notably far from the $\mathcal{P}$-points, or pass close to remarkably few $\mathcal{P}$-points. The bottom two pictures in Figure 9 depict 78 such lines, picked up by a similar procedure from the ordered list of local minima as we did above for the maxima. There are remarkably many lines that avoid passing close to $\mathcal{P}$-points, even if the lines pass right through middle of the cloud of $\mathcal{P}$-points.

The author tried the same procedure of finding regression lines on simplest random clouds of points with similar distribution, but the results are much less spectacular.

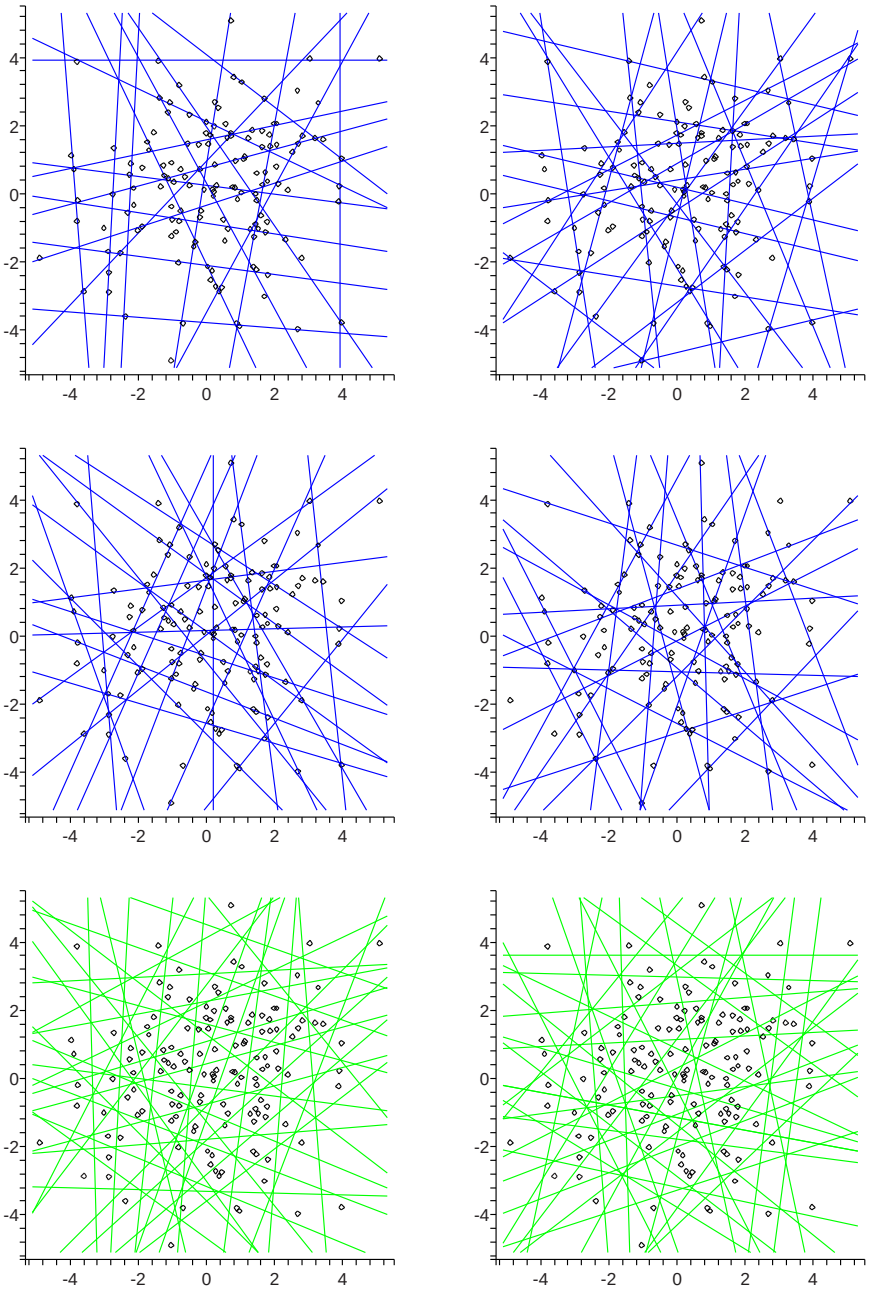

Figure 9: Linear regressions for consecutive NAO values

4 Conclusions

In Section 2 we looked at the distribution of NAO values by several means, and distinguished the set Σ in (1) of most persistent NAO values. The approximating distribution graph on the left-hand side of Figure 3 clearly shows standout maximal concentrations of NAO values. The NAO values with the standout concentrations coincide with the set Σ, except that the maximum at 1.4 is not clearly distinguishable from the nearby peak 1.7. The main maxima can be approximately noticed in the histogram on the right-hand side of Figure 3, or more conclusively, in the aggregate diagram of local maxima of all quantile histograms with 5 to 30 tallied classes in Figure 4. Finally, we investigated a diagram of shortest intervals with 4 to 40 NAO values in Figure 5; the diagram indicates all exceptional values in Σ rather convincingly. Higher concentrations of NAO values at the set Σ most probably indicates attractors or Lagrangian points of the underlying dynamical system.

In Section 3 we investigate the degree of dependence of consecutive NAO values. Figure 8 shows that the distributions of differences and sums of pairs of consecutive NAO values deviate from Gaussian normal distribution significantly — there are standout maxima and minima as well. The distribution graphs for 3-4-or-5 year averages in Figure 7 show no sign of averaging distribution discrepancies out, which shows certain measure of dependence between the consecutive NAO values. Finally, we looked at most frequently occurring first order linear regressions of consecutive NAO values, and find remarkably many of them; see the first 4 pictures in Figure 9, and compare them with the bottom 2 pictures of "anti-regression" lines for consecutive NAO values. These observations suggest not only persisting "attractor" regimes, but also dominant linear regressions (of first order) for climate transitions from year to year. Very possibly, different dynamical mechanisms dominate transitions between different years, and several transitional modes may occur regularly or frequently. Further analysis may show which linear regressions delimited in Section 3 are more likely to be substantial, how they change throughout decades, and how they relate to behavior of other climate time series.

More definite conclusions can be made after applying our statistical methods to other climate time series. In particular, it would be interesting to observe correlations between persistent values of different time series, persistent linear regressions between different climate time series, or coincidences of the same persistent transitions from several climate time series. Relevant time series could be the following: annual station based NAO index [3], Arctic seasonal or annual mean temperatures [4], annual Atlantic hurricane activity data [5]. The simple statistical methods of this paper should also be tested on suitably generated random time series.

References

[1] T. Hastie, R. Tibshirani, J. Friedman, *The Elements of Statistical Learning*, Springer, 2003.

[2] J.W. Hurrell, Y. Kushnir, G. Ottersen, and M. Visbeck (Eds.), *The North Atlantic Oscillation: Climatic Significance and Environmental Effect*, 2003. Geophysical Monograph Series, 134, 279pp.

[3] J.W. Hurrell, *Climate Indices –> Winter (Dec-Mar) Station Based NAO Index*, the websites http://www.cgd.ucar.edu/cas/jhurrell/indices.html and http://www.cgd.ucar.edu/cas/jhurrell/nao.stat.winter.html

[4] Goddard Institute for Space Studies, *GISS Surface Temperature Analysis*, the website http://data.giss.nasa.gov/gistemp/.

[5] National Weather Service, National Hurricane Center, *Tropical Cyclone Climatology*, the website http://www.nhc.noaa.gov/pastprofile.shtml.

[6] C.C. Raible, C. Casty, J. Luterbacher, A. Pauling, J. Esper, D.C. Frank, U. Büntgens, A.C. Roesch, M. Wild, P. Tschuck, P.-L. Vidale, C. Schr, H. Wanner, *Climate Variability - Observations, Reconstructions and Model Simulations*, to appear in Clim. Change., 2005.

List of MHF Preprint Series, Kyushu University

21st Century COE Program
Development of Dynamic Mathematics with High Functionality

MHF2003-1 Mitsuhiro T. NAKAO, Kouji HASHIMOTO & Yoshitaka WATANABE
A numerical method to verify the invertibility of linear elliptic operators with applications to nonlinear problems

MHF2003-2 Masahisa TABATA & Daisuke TAGAMI
Error estimates of finite element methods for nonstationary thermal convection problems with temperature-dependent coefficients

MHF2003-3 Tomohiro ANDO, Sadanori KONISHI & Seiya IMOTO
Adaptive learning machines for nonlinear classification and Bayesian information criteria

MHF2003-4 Kazuhiro YOKOYAMA
On systems of algebraic equations with parametric exponents

MHF2003-5 Masao ISHIKAWA & Masato WAKAYAMA
Applications of Minor Summation Formulas III, Plücker relations, Lattice paths and Pfaffian identities

MHF2003-6 Atsushi SUZUKI & Masahisa TABATA
Finite element matrices in congruent subdomains and their effective use for large-scale computations

MHF2003-7 Setsuo TANIGUCHI
Stochastic oscillatory integrals - asymptotic and exact expressions for quadratic phase functions -

MHF2003-8 Shoki MIYAMOTO & Atsushi YOSHIKAWA
Computable sequences in the Sobolev spaces

MHF2003-9 Toru FUJII & Takashi YANAGAWA
Wavelet based estimate for non-linear and non-stationary auto-regressive model

MHF2003-10 Atsushi YOSHIKAWA
Maple and wave-front tracking — an experiment

MHF2003-11 Masanobu KANEKO
On the local factor of the zeta function of quadratic orders

MHF2003-12 Hidefumi KAWASAKI
Conjugate-set game for a nonlinear programming problem

MHF2004-1 Koji YONEMOTO & Takashi YANAGAWA
Estimating the Lyapunov exponent from chaotic time series with dynamic noise

MHF2004-2 Rui YAMAGUCHI, Eiko TSUCHIYA & Tomoyuki HIGUCHI
State space modeling approach to decompose daily sales of a restaurant into time-dependent multi-factors

MHF2004-3 Kenji KAJIWARA, Tetsu MASUDA, Masatoshi NOUMI, Yasuhiro OHTA & Yasuhiko YAMADA
Cubic pencils and Painlevé Hamiltonians

MHF2004-4 Atsushi KAWAGUCHI, Koji YONEMOTO & Takashi YANAGAWA
Estimating the correlation dimension from a chaotic system with dynamic noise

MHF2004-5 Atsushi KAWAGUCHI, Kentarou KITAMURA, Koji YONEMOTO, Takashi YANAGAWA & Kiyofumi YUMOTO
Detection of auroral breakups using the correlation dimension

MHF2004-6 Ryo IKOTA, Masayasu MIMURA & Tatsuyuki NAKAKI
A methodology for numerical simulations to a singular limit

MHF2004-7 Ryo IKOTA & Eiji YANAGIDA
Stability of stationary interfaces of binary-tree type

MHF2004-8 Yuko ARAKI, Sadanori KONISHI & Seiya IMOTO
Functional discriminant analysis for gene expression data via radial basis expansion

MHF2004-9 Kenji KAJIWARA, Tetsu MASUDA, Masatoshi NOUMI, Yasuhiro OHTA & Yasuhiko YAMADA
Hypergeometric solutions to the q - Painlevé equations

MHF2004-10 Raimundas VIDŪNAS
Expressions for values of the gamma function

MHF2004-11 Raimundas VIDŪNAS
Transformations of Gauss hypergeometric functions

MHF2004-12 Koji NAKAGAWA & Masakazu SUZUKI
Mathematical knowledge browser

MHF2004-13 Ken-ichi MARUNO, Wen-Xiu MA & Masayuki OIKAWA
Generalized Casorati determinant and Positon-Negaton-Type solutions of the Toda lattice equation

MHF2004-14 Nalini JOSHI, Kenji KAJIWARA & Marta MAZZOCCO
Generating function associated with the determinant formula for the solutions of the Painlevé II equation

MHF2004-15 Kouji HASHIMOTO, Ryohei ABE, Mitsuhiro T. NAKAO & Yoshitaka WATANABE
Numerical verification methods of solutions for nonlinear singularly perturbed problem

MHF2004-16 Ken-ichi MARUNO & Gino BIONDINI
Resonance and web structure in discrete soliton systems: the two-dimensional Toda lattice and its fully discrete and ultra-discrete versions

MHF2004-17 Ryuei NISHII & Shinto EGUCHI
Supervised image classification in Markov random field models with Jeffreys divergence

MHF2004-18 Kouji HASHIMOTO, Kenta KOBAYASHI & Mitsuhiro T. NAKAO
Numerical verification methods of solutions for the free boundary problem

MHF2004-19 Hiroki MASUDA
Ergodicity and exponential β-mixing bounds for a strong solution of Lévy-driven stochastic differential equations

MHF2004-20 Setsuo TANIGUCHI
The Brownian sheet and the reflectionless potentials

MHF2004-21 Ryuei NISHII & Shinto EGUCHI
Supervised image classification based on AdaBoost with contextual weak classifiers

MHF2004-22 Hideki KOSAKI
On intersections of domains of unbounded positive operators

MHF2004-23 Masahisa TABATA & Shoichi FUJIMA
Robustness of a characteristic finite element scheme of second order in time increment

MHF2004-24 Ken-ichi MARUNO, Adrian ANKIEWICZ & Nail AKHMEDIEV
Dissipative solitons of the discrete complex cubic-quintic Ginzburg-Landau equation

MHF2004-25 Raimundas VIDŪNAS
Degenerate Gauss hypergeometric functions

MHF2004-26 Ryo IKOTA
The boundedness of propagation speeds of disturbances for reaction-diffusion systems

MHF2004-27 Ryusuke KON
Convex dominates concave: an exclusion principle in discrete-time Kolmogorov systems

MHF2004-28 Ryusuke KON
Multiple attractors in host-parasitoid interactions: coexistence and extinction

MHF2004-29 Kentaro IHARA, Masanobu KANEKO & Don ZAGIER
Derivation and double shuffle relations for multiple zeta values

MHF2004-30 Shuichi INOKUCHI & Yoshihiro MIZOGUCHI
Generalized partitioned quantum cellular automata and quantization of classical CA

MHF2005-1 Hideki KOSAKI
Matrix trace inequalities related to uncertainty principle

MHF2005-2 Masahisa TABATA
Discrepancy between theory and real computation on the stability of some finite element schemes

MHF2005-3 Yuko ARAKI & Sadanori KONISHI
Functional regression modeling via regularized basis expansions and model selection

MHF2005-4 Yuko ARAKI & Sadanori KONISHI
Functional discriminant analysis via regularized basis expansions

MHF2005-5 Kenji KAJIWARA, Tetsu MASUDA, Masatoshi NOUMI, Yasuhiro OHTA & Yasuhiko YAMADA
Point configurations, Cremona transformations and the elliptic difference Painlevé equations

MHF2005-6 Kenji KAJIWARA, Tetsu MASUDA, Masatoshi NOUMI, Yasuhiro OHTA & Yasuhiko YAMADA
Construction of hypergeometric solutions to the q - Painlevé equations

MHF2005-7 Hiroki MASUDA
Simple estimators for non-linear Markovian trend from sampled data:
I. ergodic cases

MHF2005-8 Hiroki MASUDA & Nakahiro YOSHIDA
Edgeworth expansion for a class of Ornstein-Uhlenbeck-based models

MHF2005-9 Masayuki UCHIDA
Approximate martingale estimating functions under small perturbations of dynamical systems

MHF2005-10 Ryo MATSUZAKI & Masayuki UCHIDA
One-step estimators for diffusion processes with small dispersion parameters from discrete observations

MHF2005-11 Junichi MATSUKUBO, Ryo MATSUZAKI & Masayuki UCHIDA
Estimation for a discretely observed small diffusion process with a linear drift

MHF2005-12 Masayuki UCHIDA & Nakahiro YOSHIDA
AIC for ergodic diffusion processes from discrete observations

MHF2005-13 Hiromichi GOTO & Kenji KAJIWARA
Generating function related to the Okamoto polynomials for the Painlevé IV equation

MHF2005-14 Masato KIMURA & Shin-ichi NAGATA
Precise asymptotic behaviour of the first eigenvalue of Sturm-Liouville problems with large drift

MHF2005-15 Daisuke TAGAMI & Masahisa TABATA
Numerical computations of a melting glass convection in the furnace

MHF2005-16 Raimundas VIDŪNAS
Normalized Leonard pairs and Askey-Wilson relations

MHF2005-17 Raimundas VIDŪNAS
Askey-Wilson relations and Leonard pairs

MHF2005-18 Kenji KAJIWARA & Atsushi MUKAIHIRA
Soliton solutions for the non-autonomous discrete-time Toda lattice equation

MHF2005-19 Yuu HARIYA
Construction of Gibbs measures for 1-dimensional continuum fields

MHF2005-20 Yuu HARIYA
Integration by parts formulae for the Wiener measure restricted to subsets in $\mathbb{R}^d$

MHF2005-21 Yuu HARIYA
A time-change approach to Kotani's extension of Yor's formula

MHF2005-22 Tadahisa FUNAKI, Yuu HARIYA & Mark YOR
Wiener integrals for centered powers of Bessel processes, I

MHF2005-23 Masahisa TABATA & Satoshi KAIZU
Finite element schemes for two-fluids flow problems

MHF2005-24 Ken-ichi MARUNO & Yasuhiro OHTA
Determinant form of dark soliton solutions of the discrete nonlinear Schrödinger equation

MHF2005-25 Alexander V. KITAEV & Raimundas VIDŪNAS
Quadratic transformations of the sixth Painlevé equation

MHF2005-26 Toru FUJII & Sadanori KONISHI
Nonlinear regression modeling via regularized wavelets and smoothing parameter selection

MHF2005-27 Shuichi INOKUCHI, Kazumasa HONDA, Hyen Yeal LEE, Tatsuro SATO, Yoshihiro MIZOGUCHI & Yasuo KAWAHARA
On reversible cellular automata with finite cell array

MHF2005-28 Toru KOMATSU
Cyclic cubic field with explicit Artin symbols

MHF2005-29 Mitsuhiro T. NAKAO, Kouji HASHIMOTO & Kaori NAGATOU
A computational approach to constructive a priori and a posteriori error estimates for finite element approximations of bi-harmonic problems

MHF2005-30 Kaori NAGATOU, Kouji HASHIMOTO & Mitsuhiro T. NAKAO
Numerical verification of stationary solutions for Navier-Stokes problems

MHF2005-31 Hidefumi KAWASAKI
A duality theorem for a three-phase partition problem

MHF2005-32 Hidefumi KAWASAKI
A duality theorem based on triangles separating three convex sets

MHF2005-33 Takeaki FUCHIKAMI & Hidefumi KAWASAKI
An explicit formula of the Shapley value for a cooperative game induced from the conjugate point

MHF2005-34 Hideki MURAKAWA
A regularization of a reaction-diffusion system approximation to the two-phase Stefan problem

MHF2006-1 Masahisa TABATA
Numerical simulation of Rayleigh-Taylor problems by an energy-stable finite element scheme

MHF2006-2 Ken-ichi MARUNO & G R W QUISPEL
Construction of integrals of higher-order mappings

MHF2006-3 Setsuo TANIGUCHI
On the Jacobi field approach to stochastic oscillatory integrals with quadratic phase function

MHF2006-4 Kouji HASHIMOTO, Kaori NAGATOU & Mitsuhiro T. NAKAO
A computational approach to constructive a priori error estimate for finite element approximations of bi-harmonic problems in nonconvex polygonal domains

MHF2006-5 Hidefumi KAWASAKI
A duality theory based on triangular cylinders separating three convex sets in R^n

MHF2006-6 Raimundas VIDŪNAS
Uniform convergence of hypergeometric series

MHF2006-7 Yuji KODAMA & Ken-ichi MARUNO
N-Soliton solutions to the DKP equation and Weyl group actions

MHF2006-8 Toru KOMATSU
Potentially generic polynomial

MHF2006-9 Toru KOMATSU
Generic sextic polynomial related to the subfield problem of a cubic polynomial

MHF2006-10 Shu TEZUKA & Anargyros PAPAGEORGIOU
Exact cubature for a class of functions of maximum effective dimension

MHF2006-11 Shu TEZUKA
On high-discrepancy sequences

MHF2006-12 Raimundas VIDŪNAS
Detecting persistent regimes in the North Atlantic Oscillation time series